A New Standard: RHIDE versus conventional techniques in evaluating wheelchair propulsion related biomechanics

Puck Willemse

Summary

This thesis discusses the potential of the RHIDE system, a device designed to measure in-field wheelchair handrim push characteristics. The research question is if the RHIDE can accurately discriminate propulsion/recovery and determine contact/release angles. This research question is answered by determining push time (τ), contact angle (α), release angle (β) and push time (Δ) for each push. To validate the RHIDE, these biomechanics are measured with two different systems, one being the RHIDE and the other being the Marker-Less and Machine Learning Vision System (MLVS). Validation is conducted using data from an experiment comprising 12 wheelchair propulsion-related tests on an ergometer, with variations in speed (S1 and S2) and resistance (R1 and R2). For every push, τ, α, β and Δ are extracted with both systems and the reliability of the RHIDE is calculated using an ICC(2,1) on absolute agreement of the biomechanics for all pushes. For τ, ICC values are 0.65 for S1R1, 0.88 for S1R2, 0.98 S2R1 and 0.96 for S2R2 therefore reliability is considered moderate, good, excellent and excellent respectively. For α, ICC values are 0.67 for S1R1, 0.59 for S1R2, 0.56 S2R1 and 0.51 for S2R2 giving moderate reliability for all tests. The β ICC values are 0.57 for S1R1, 0.34 for S1R2, 0.35 S2R1 and 0.26 for S2R2 giving poor reliability for all tests except S1R1. At last, Δ ICC values are 0.17 for S1R1, 0.52 for S1R2, 0.25 S2R1 and 0.14 for S2R2, giving poor reliability for all tests except S1R2. Overall, the RHIDE is able to accurately discriminate propulsion/recovery phases. Touch/release angles are not reliable between systems. There are two potential causes for this. Firstly, the RHIDE could improve its accuracy by increasing sample rate, streamline data pathways and the introduction of a calibration protocol. Secondly, both systems measure different contact/release angles and are therefore not comparable in this matter.

Overall, RHIDE has the potential to occupy a unique position in wheelchair propulsion analysis by enabling the measurement of daily activities. With RHIDE, it would be feasible to (1) provide information about propulsion technique by supplying push/release angles and push times and (2) offer insights into daily wheelchair use over extended periods.

Chapter 1

Introduction

In 1948 the first wheelchair sporting event called 'Games' was organized for disabled British veterans. The Games developed into an international wheelchair sporting competition and joined the paralympics in 1960, causing the sport to gain attention. An increase in popularity led to more specialized equipment and an increase in athletes that began to train for these competitions. This progressed until the early 1980s, when athletes began to use more sophisticated equipment and training techniques as stated by Cooper [1990]. As a consequence, publications such as Wolfe et al. [1977] and Van Der Woude et al. [1989] started quantifying components of wheelchair propulsion technique which allowed for comparison between wheelchair users (WCU). As WCU propulsion research continued, different aspects of WCU biomechanics were explored [Sanderson and Sommer, 1985], [Veeger et al., 1991] & [van der Woude et al., 1989].

Chow and Levy [2011] clarify that most studies focus on results in one or more of the following areas: 'kinematic', 'kinetic' or 'timing and muscle activation'. Kinematics biomechanics focus on describing the propulsion motion of a WCU. To do this, propulsion is generally broken down into individual pushes allowing the measurement of biomechanics such as push frequency. Every push is also divided into different phases: a (1) propulsion phase and a (2) recovery phase. Chow and Levy [2011] summarize the most used kinematics biomechanics, which are:

- Distance travelled per push

- Average speed

- Stroke frequency

- Time and percentage spent in each propulsion/recovery phase (push/recovery time)

- Angle where the propulsion/recovery phase starts (touch/recovery angle, recovery angle will be called release angle throughout this thesis)

- Difference between propulsion angle and recovery angle (push angle)

.

Kinematic biomechanics are commonly measured with motion capture. However, this method is time intensive and not flexible to set-up. Because of these difficulties, most experiments with motion capture are executed in a controlled environment such as a laboratory. This makes motion capture unfit to acquire kinematic biomechanics in daily life, which is assumed to be a major limitation for progression within the field of wheelchair biomechanics as stated by de Vries et al. [2023]. To overcome the limitations that come with motion capture, this paper will test a novel system called the Rim Hit Detection (RHIDE). The RHIDE consists of a sleeve that can be installed on a wheelchair push-rim, in which multiple electrodes are integrated in combination with an Inertia Measurement Unit (IMU) around the wheel axle. The electrodes detect touch and the IMU provides rotation, acceleration and magnetic field data. The combination of touch location combined with the IMU allows the calculations of kinematic biomechanics such as push time, touch/release angle while allowing for automatized data processing due to the simple design of the RHIDE.

The hypothesis is that the RHIDE should provide enough information to discriminate between the propulsion/release phase and determine the push angles of the user. If this is the case, kinematic biomechanics can be measured without the use of motion capture. More flexible measuring set-ups enable possibilities such as measuring propulsion technique of WCU in their daily life without the need of a laboratory. Being able to track daily wheelchair behavior would open up many possibilities for research. To give some ideas, the RHIDE would be able to (1) provide an approximate calorie count and push count for daily wheelchair users, (2) give information about propulsion technique to physiotherapists by providing push/release angles and push times and (3) allow researchers to gather daily wheelchair use information over longer periods of time.

As made clear by Yves et al. [2001] and Bakatchina et al. [2021], the definition of propulsion/release phase varies per study. Researchers using the motion capture approach generally define the propulsion phase based on visual contact with the rim, while other researchers define the propulsion phase based on applied force. Since the RHIDE will be compared to an optoelectronic approach, in this paper, the propulsion phase is defined as the phase in which hand contact is detected for at least 0.05s. The research question of this paper is: Can the RHIDE-system discriminate propulsion/release phase and provide contact/release angles, with a similar accuracy compared to the tools that are currently used? This will be assessed by the ICC score rating suggested by Koo and Li [2016] on absolute agreement of biomechanics acquired via the RHIDE versus biomechanics acquired via optoelectronic. Complimentary to the research question, possibilities and limitations of the RHIDE will be explored.

Chapter 2

Method

To test the RHIDE performance, a set of experiments have been performed on a ergometer. Participants had to perform multiple propulsion protocols while being measured with two systems that both are used to calculate kinematic biomechanics. For every push, the following kinematic biomechanics are extracted: push time, contact angle, release angle. Push time (τ) is the time difference between the start of a push τ_1 and the release of a push τ_2. Angles are represented clockwise and relative to 12h, where the contact angle α is the angle representing the touch location at τ_1 and the release angle β is the angle representing the release location at τ_2. Push angle (Δ) is the netto angle of the push, which is calculated by $\Delta = \beta - \alpha$. Symbols shown schematically in figure 2.1.
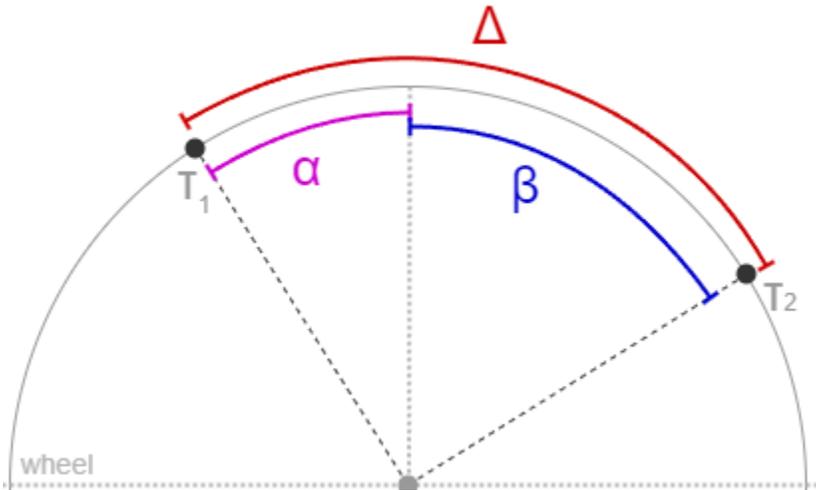
Figure 2.1: Schematic display of a wheel with contact time/point τ_1 and τ_2. Push time (τ) is the time between τ_1 and τ_2 in (s). Contact angle (α) is the angle representing the touch location at τ_1 in (°) relative to 12h. release angle (β) is the angle representing the touch location at τ_2 in (°) relative to 12h. Push angle (Δ) is the netto angle ($\beta - \alpha$).

2.1 Sensors

The RHIDE-system consists of two sensors. The first being an array of 24 capacitive sleeves connected to a PVC hose that can be clamped to a wheelchair rim, as shown in Figure 2.2. The capacitive sleeves are connected to two sensor modules (MPR121) to measure contact proximity. This system has a sample rate of 29.4 Hz. The second sensor is an Inertia Measurement Unit, which is the NGIMU from X-io Technologies [2024], that provides three dimensional angular velocity, three-dimensional linear acceleration, local orientation and time stamps with a sample rate of 50 Hz. A microcontroller extracts contact data from the MPR121 and sends this to the NGIMU which adds a timestamp. Consecutively, the NGIMU can be read through WiFi. The capacitive sleeves are connected to the rim of the right wheel. The microcontroller and IMU are connected near the centre of the wheel, as can be seen in Figure 2.3. All and all, raw data of the RHIDE consists of: touch proximity of 24 electrode values over time (29.4 Hz), 3D gyroscope, accelerometer, magnetometer, barometer and quaternions over time (50 Hz).

A second system called the MLVS (Marker-Less and Machine Learning Vision System), consist of a camera which is placed on the right side of the participant. An important part of the MLVS is the algorithm that is applied to the frames. This algorithm is being developed to detect hand contact with the rim. However, for this thesis, using the algorithm is out of scope and therefore only the raw camera frames are used. The camera collects 848×480 RGB frames (60 Hz) and is placed at approximately 1.0 m from the subject, giving a resolution of 1.5 mm/pixel. Figure 2.3 is created with a frame from this camera, showing the camera orientation relative to the experiment setup.

The tests have been performed on an Asseda ergometer [de Klerk et al., 2020], which is a wheelchair ergometer consisting of two motor controlled rollers. The wheelchair is held in place with its wheels onto the rollers. When a force is applied to the wheelchair wheels, this is measured in the rollers. The rollers then react by turning according to the applied force, providing active forces (100 Hz). In this thesis, the active forces are not utilized.

2.2 Protocol

21 non-disabled, inexperienced participants (22.3 years $\pm$ 1.8 years) performed multiple push related tasks while being measured with the camera, RHIDE and ergometer. To simulate different circumstances of wheelchair propulsion each participant performed four different tests. The order of these tests was randomized per participant and the tests consisted of the following settings:

- Target speed of 4 km/h with a rolling resistance coefficient of 0.000 for 60s (S1R1).

- Target speed of 4 km/h with a rolling resistance coefficient of 0.008 for 60s (S1R2).

- Full sprint with a rolling resistance coefficient of 0.000 for 10s (S2R1).

- Full sprint with a rolling resistance coefficient of 0.008 for 10s (S2R2).

Each test started and ended with a short synchronization protocol where the participant was asked to rotate the wheel forth and back three times without detaching the hand from the push-rim. After the first synchronization protocol, the participant was given a brief moment before one of the above mentioned tests had to be performed. After that test, an instructor explained when to perform the second calibration protocol. Participants were informed about the aims and procedure of the study before the conditions and signed informed consent. The study had been performed according to the guidelines of the ethical committee of the centre Human Movement Sciences identified with code R201900802, University Medical Center Groningen (ECB_202000706).
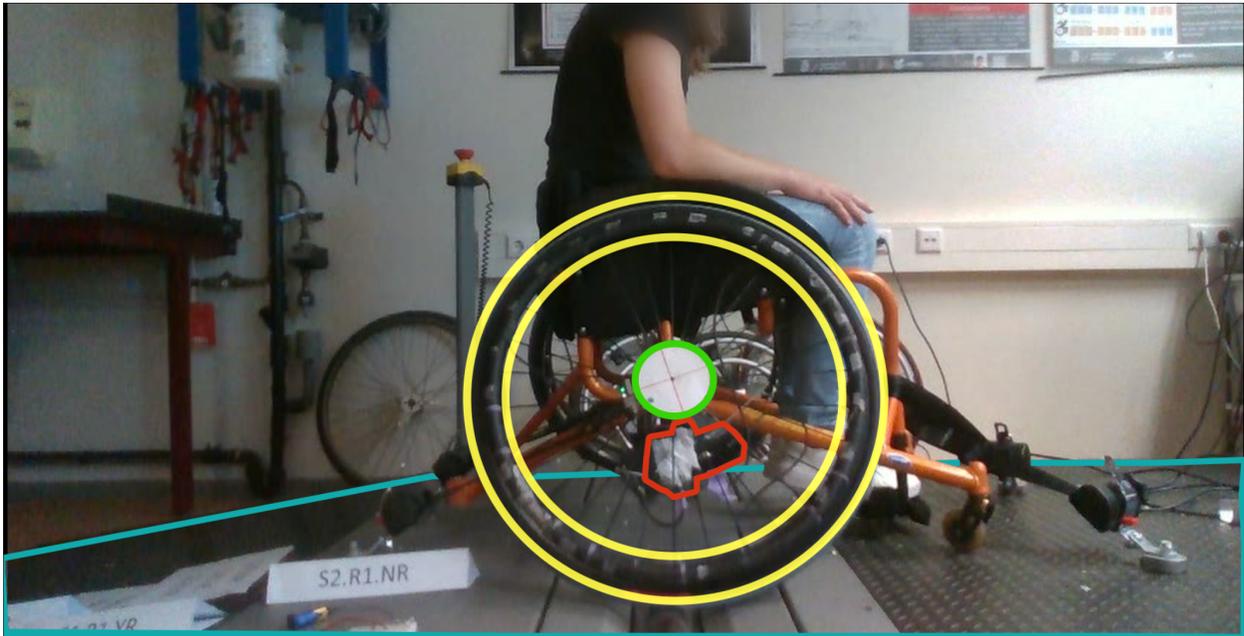
Figure 2.2: Overview of the experiment setup with the ergometer, the RHIDE consisting of the sleeve with electrodes & the IMU/microcontroller and the center of the wheel for the camera. This image is a frame from the MLVS camera.

2.3 Pre-processing

The RHIDE system exports 24 electrode values in one string per time instance. To separate the different electrodes into numerical values, the code displayed in the appendix 5.1 is used. Afterwards, the numerical values were further normalized by fitting the MinMax Scaler by Pedregosa et al. [2011] on the whole dataset. The transformation of this fit is applied to individual measurements to normalize electrode values, making it easier to apply general rules for all electrodes.
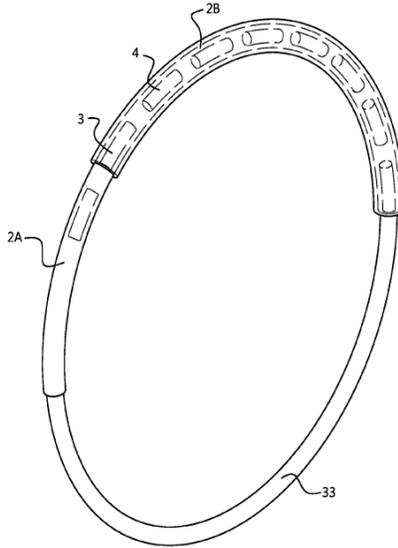
Figure 2.3: Overview of the capacitive sleeves of the RHIDE system attached to a wheelchair rim, indicated by 33. 2A and 2B both indicate an isolation layer. Both 3 and 4 are electrodes that detect touch. There are 24 electrodes distributed around the rim.

2.4 Data extraction

The goal is to compare push times and contact/release angles for individual pushes. Both the RHIDE and video require data processing to acquire these biomechanics.

2.4.1 RHIDE

To get from touch proximity and IMU data to push time, contact and release angles for every push, several steps have to be taken. These steps consist of determining:

- Contact

- Pushes

- Wheel orientation

Firstly, contact is determined based on values from all electrodes. As all electrode values are normalized, a general threshold is set to discriminate between contact and non-contact, expressed in a touch boolean. As electrode drift varied per electrode, the threshold compensated for this. The formula for the threshold per electrode is the following:

$$X_n = X_{flat} + 2d_n \tag{2.1}$$

where X_n is the threshold value for an individual electrode (n), X_{flat} is a set value & d_n is the drift of electrode n measured at the last 5 seconds of a measurement. An example of the touch boolean feature is shown in figure 2.4.
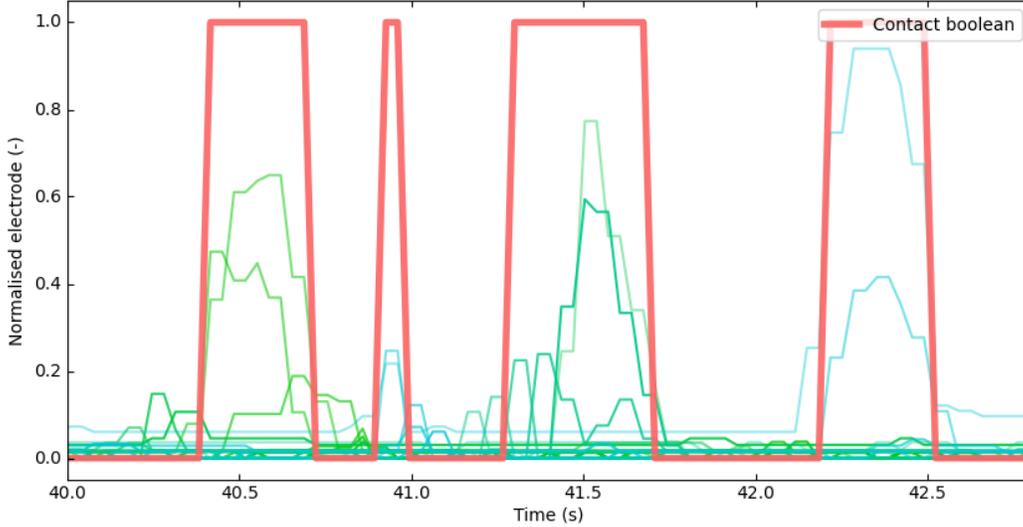
Figure 2.4: Example of the contact boolean on a small part of a randomly selected measurement. The green/blue lines are 24 individual electrodes and the red line displays the touch boolean based on all these 24 electrodes. In this example is X_{flat} set to 0.2. A value of 1 means that touch is detected.

The second step in the data extraction is determining which contacts are pushes, which are accidental touches and the touch location (T_L) of a push. Contact can only be considered a push if contact is detected for more than 3 samples ($\approx$ 0.05s). Contacts longer than 3 samples will go through a function that determines the T_L of that contact. T_L is a float value between 0 - 24 representing the electrodes of the RHIDE. As the electrode signal is proportional to the touched surface area of that electrode, the T_L is calculated based on the relative surface area of the electrodes signals within a push. Details can be found in the code located in the appendix 5.2.

Finally, with the knowledge of which touches are pushes and where contact is made within that push, the push time and contact/release angles can be calculated. Push time is calculated by taking the time difference of the beginning and the end of the push. Contact/release angles are calculated by using the following formula at the time of contact/release:

$$q_{angle} = q_{loc} \cdot q_{offset} \cdot q_{push} \cdot q_{global}^{-1} \tag{2.2}$$

where q_{angle} is the quaternion representing the contact angle. q_{loc} is acquired directly from the IMU using the Madgwick filter [Madgwick, 2010] and represents the quaternion of the (local) IMU orientation. q_{global} is a constant quaternion representing another local orientation that is used to project q_{loc} in the 2D plane of the wheel by multiplying q_{loc} with the inverse of q_{global}. The other quaternions both represent offset angles in the plane of the wheel. As every electrode covers 15°, q_{push} is calculated by multiplying T_L with 15 and applying that rotation to the plane of the wheel. Lastly, q_{offset} is a constant quaternion used to calibrate the local frame to the global frame. In the used dataset it is impossible to determine q_{offset}

7

based on IMU data only. Without q_{offset}, only relative angles are accurate. This is solved by using the video data to calibrate the RHIDE system, by choosing q_{offset} such that the second RHIDE contact angle is equal to the second video contact angle. Details can be found in the appendix 5.3. As all quaternions are projected into a 2D space, the contact/release angle can be calculated directly by taking the angle of q_{angle}.

2.4.2 Video

To acquire push time, contact and release angles based on the video data, an algorithm has been written that allows a user to go through a video frame by frame, select the centre of the wheel and click at the point of contact or release. Contact/release pixel coordinates are converted to vectors which are used to calculate the contact/release angles. Push time is calculated by dividing the number of frames between touch and release through the frame rate of the video.

2.5 Data analysis

As the manual video extraction of biomechanics is a time consuming task, a random sub-selection of 12 tests is made. The sub-selection is ensured to consist of 3 S1R1, 3 S1R2, 3 S2R1 & 3 S2R2 tests. The RHIDE and video data is synchronized by matching the timing of the first and last push. Both systems extracted push times and contact/release angles for every push on every performed tests. Pushes from both systems are matched by taking the nearest push (timewise) extracted by the RHIDE for every push extracted by video.

Results are presented by plotting biomechanics of every push measured with the two systems. Within the plots, results are separated based on the performed tests. The agreement of the systems is statistically determined by calculating ICC representing the two-way random effects, absolute agreement, single rater/measurement model as defined by McGraw and Wong [1996]. This model, also called ICC(2,1), is applied by using 'intraclass_corr' function [Vallat, 2018] giving the absolute agreement of both sensors for every parameter.

Chapter 3

Results

In the results, RHIDE results have subscript 'RH' and video results have subscript 'V'. Overall 497 pushes have been found based on the video and 500 pushes with the RHIDE. From these results, five pushes were only found by the RHIDE and three pushes were only found by the video.

Push times, contact angles, release angles and push angles are plotted for all pushes in figure 3.1, figure 3.2, figure 3.3 & figure 3.4 respectively. Table 3.1 shows the ICC(2,1) for all parameters for every test acquired via intraclass_corr function from Vallat [2018].
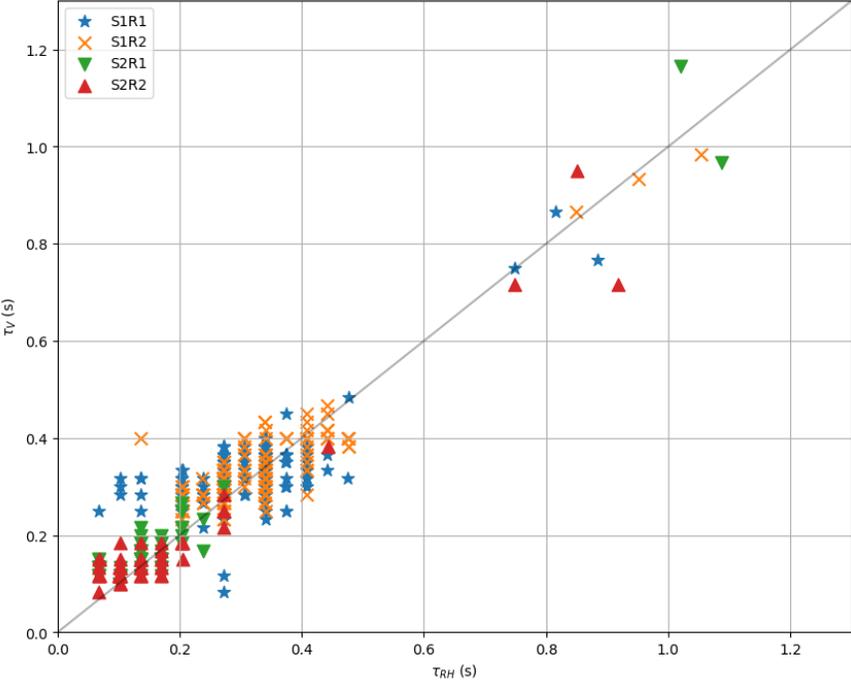
Figure 3.1: Push times measured with both the RHIDE (τ_{RH}) and with the video (τ_V) for every push separated per test.
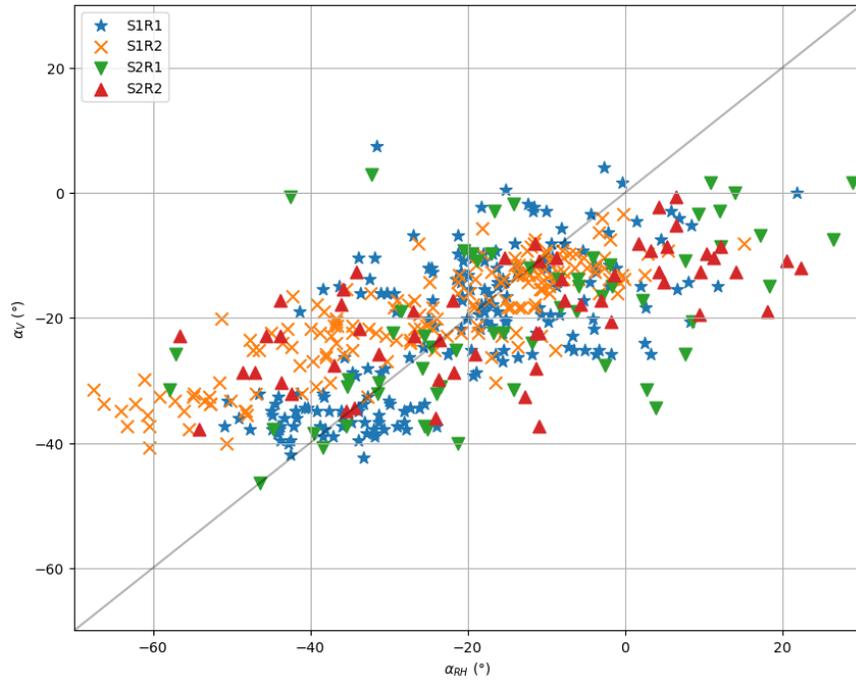
Figure 3.2: Contact angle measured with both the RHIDE (α_{RH}) and with the video (α_V) for every push separated per test.
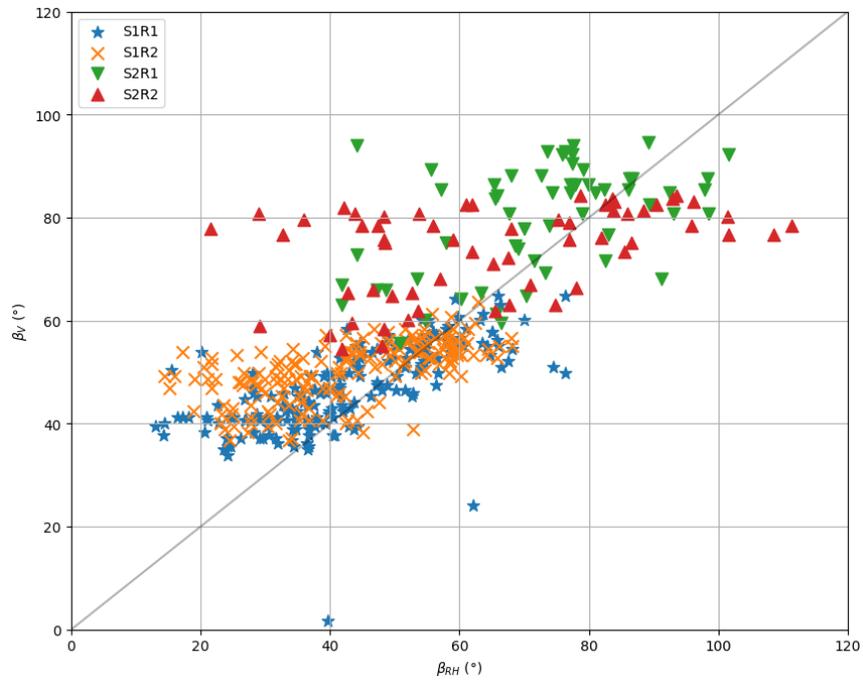
Figure 3.3: Release angle measured with both the RHIDE (β_{RH}) and with the video (β_V) for every push separated per test.

	τ	α	β	Δ
$S1R1$	0.65	0.67	0.57	0.17
$S1R2$	0.88	0.59	0.34	0.52
$S2R1$	0.98	0.56	0.35	0.25
$S2R2$	0.96	0.51	0.26	0.14

Table 3.1: ICC(2,1) absolute agreement values for the measured biomechanics τ, α, β & Δ extracted via RHIDE and video for all tests.
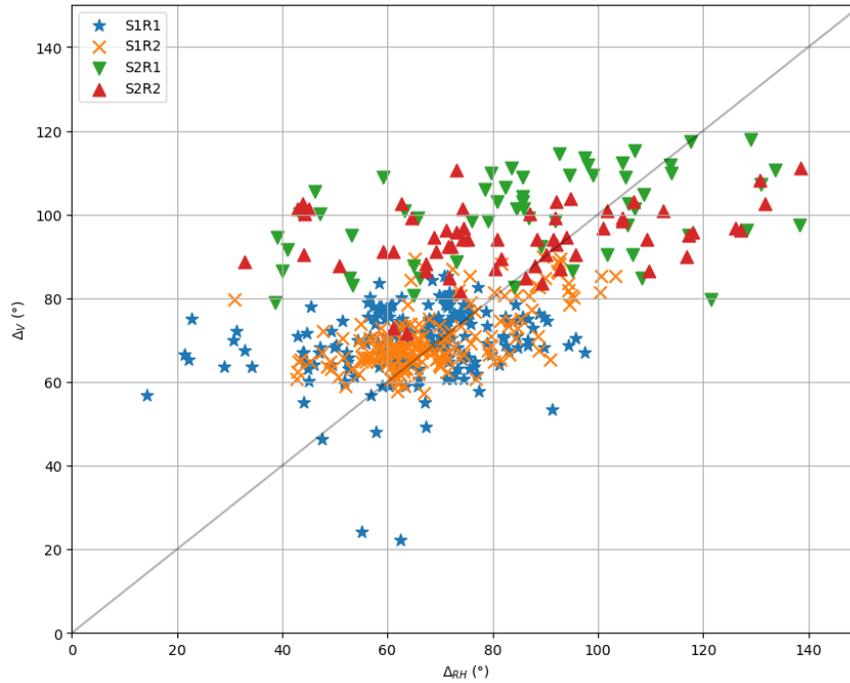
Figure 3.4: Push angle measured with both the RHIDE (Δ_{RH}) and with the video (Δ_V) for every push separated per test.

Chapter 4

Discussion

The research question consists of two parts. The first being about the discrimination of propulsion and recovery phases. As push time represents the time of the propulsion phase, it is directly related to the discrimination of both phases. As the ICC values for push times are 0.65 for S1R1, 0.88 for S1R2, 0.98 S2R1 and 0.96 for S2R2, reliability is considered moderate, good, excellent and excellent respectively [Koo and Li, 2016]. As the propulsion phases match, the recovery phases must also match, meaning that the RHIDE gives moderate to excellent results for the discrimination between propulsion/recovery phase.

A second part of the research question is if the RHIDE can provide reliable contact/release angles. The touch angle ICC values are all between 0.50 - 0.75 which indicates moderate reliability for all tests. The release angle ICC values were <0.50 indicating poor reliability for all tests except the ICC value of 0.57 for S1R1 indicating a moderate reliability. Overall, the RHIDE does not give reliable results for the touch/release angles.

An unexpectedly low ICC value is the push time for S1R1 tests. In figure 3.1 it is visible that a group of several pushes have $\tau_{RH} \approx 0.1$ while $\tau_V \approx 0.3$. A possible explanation could be that, due to the ease of low speed propulsion, the contacts made are too light and therefore do not surpass the RHIDE touch threshold. This would cause an underestimation of the τ_V which seems to be visible in figure 3.1.

Reliability of touch/release angles is expected to be lower than for push time. A first reason for this expectation is that touch/release angles rely on calibration based on one push. An offset in this calibration directly decreases the ICC value for the whole test. A second possible explanation is a relatively low sample rate of the RHIDE. At S2 measurements the wheel rotation can reach up to 500°/s making each sample around 17°. A last possible explanation could be the manual contact/release angles based on the video. Generally, α_V and β_V seem more constant than α_{RH} and β_{RH}. While the more constant values could be true, it could also be a consequence of the measuring method. Since it is difficult to determine the exact point of contact, commonly the centre of the hand is taken, which is likely not the last point of contact. Therefore, both systems might accidentally use a different definition of touch/release angle. The RHIDE determines the actual angle where contact is made. Yet, the video determines the angle of the hand location when contact is made. Another problem is the difficulty of detecting hovering versus actual contact. All in all, while the RHIDE shows more variability, there may be some truth in this variability that is neglected by acquiring angles via video.

Finally, while push/release angles are depended on calibration of the RHIDE, the push angle is not. Therefore, the push angle is expected to have a higher ICC value than the release angle. However, as can be seen in table 3.1, this is only the case for the $S1R2$ test. These results can likely be explained by the two phenomenons mentioned in the previous paragraph. Firstly, the RHIDE sample rate is too low for accurate angles at high speeds, explaining the low ICC values for $S2$ tests. Secondly, the push angle is directly related to push time. In $S1R2$, the push time ICC is relatively low, therefore it is logical that the push angle ICC is also effected. Again, the cause is likely due to light touches of a participant resulting into the touch not passing the threshold and therefore underestimating the push time for some pushes.

4.1 Limitations

A major limitation of this study is the use of an ergometer, which introduces two significant constraints. Firstly, RHIDE is designed to work in-field, which has not been tested. Introducing more degrees of freedom likely influences pushing technique and generally decreases data quality.

A second limitation concerns the current method used to calculate contact/release angles as explained in this thesis. This method does not hold up for in-field measurements. Calculating the touch/release angle based on the quaternion between two orientations does only work if the wheelchair cannot rotate. However, this can be resolved by using a different data extraction method involving Euler decomposition to acquire contact/release angles directly from the local orientation of the IMU.

Lastly, the data path of the RHIDE could be optimized. One problem is that electrode values are all collected one-by-one by the MPR121, after which they are send to the microcontroller. The microcontroller adds a time string to the string of electrode values. As the time string is added after a couple of steps, the electrode values have an effective offset around 40-60 ms. This offset has a constant value, which represents the time it takes to collect data from all electrodes and send it to the microcontroller. But the offset also has a random component due to different sample rates of the microcontroller and the IMU. The random component influences consistency of the results, effectively lowering all ICC values.

4.2 Missing information

An important part of this thesis is exploring the possibilities that RHIDE has to offer. RHIDE provides some unique opportunities that are not yet utilized. Currently, there is a lack of a calibration protocol. In this thesis, calibration is done by using video data. Calibrating the RHIDE using video data requires setting up a camera, applying data extraction of touch/release angles and synchronisation of pushes. As the RHIDE is designed to be more flexible and allow in-field measurements, calibration using video data defeats the purpose of the RHIDE.

A second opportunity that is not utilized to the full extent is the utilization of the IMU. Currently, only orientations are used while RHIDE offers more possibilities. For example,

the IMU provides rotational speeds and accelerations. This allows for a unique calibrated combination of contact moment and wheel rotational acceleration/speed.

Another opportunity lies within the touch detection capabilities of RHIDE. Currently, the results that are shown are based on a touch boolean, which only discriminates between push and non-push. While this is relevant, other types of touches detectable with RHIDE could be beneficial for future research. For example, the following touches are visible within RHIDE data: (1) hand sliding over the electrodes (Figure 4.1), (2) shifting of the hand/contact point while pushing and (3) random touches. Detecting these different touches may provide insight into user propulsion technique.
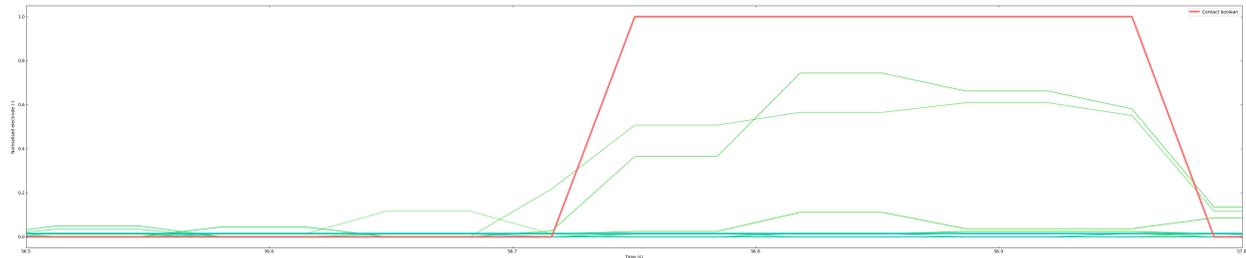
Figure 4.1: An example of the hand sliding over multiple electrodes before a push. This can be seen by the signals from different electrodes before the touch boolean is triggered.

4.3   Future outlook

Besides extracting results more easily, the real potential of RHIDE lies in its usability. It can accurately provide push time of all pushes without the need of excessive data processing. To unlock the full potential of the RHIDE, the accuracy of touch/release angles should be improved and the RHIDE should be tested on in-field measurements. Improving the accuracy can be done in two ways. Firstly, increasing the electrode sample rate, as 29.4 Hz is not enough for accurate results at higher speeds. This also reduces the random variability between the 40-60 ms offset. Secondly, streamline the electrode data pathway to remove the offset. While there will always be some offset due communication between sensors, a big part of the current offset is a constant offset. If this offset is unknown for a user, it will cause confusion and/or worse results than necessary.

4.4   Conclusion

This thesis serves as an initial pilot for the RHIDE system, focusing on comparing it to system based on video and exploring further possibilities. When comparing both systems, ICC values show that the RHIDE gives moderate- to excellent reliability for push time (τ), moderate reliability for touch angle (α), moderate- to poor reliability for release angle (β) and moderate- to poor reliability for push angle (Δ). The reliability could likely be improved by introducing a calibration protocol, increasing sample frequency and changing the electrode data path way.

Based on the push time, the RHIDE is clearly able to differentiate the push and recovery phase. This offers potential benefits such as easier data processing and more flexible experiment setups. As for determining touch/release/push angles, the ICC values are low. ICC values could likely be improved by improving sample rate, streamlining data pathways and the introduction of a calibration protocol. However, there is a possibility that both systems measure different contact/release angles, which would also effect the push angles.

All in all, while further research is needed to fully realize its potential, RHIDE demonstrates promising results. Its unique potential to measure daily wheelchair activities could offer significant benefits to daily wheelchair users, physiotherapists and researchers.

Bibliography

S. Bakatchina, T. Weissland, M. Astier, D. Pradon, and A. Faupin. Performance, asymmetry and biomechanical parameters in wheelchair rugby players. *Sports Biomechanics*, page 1–14, 2021. ISSN 1476-3141. doi: 10.1080/14763141.2021.1898670.

J. W. Chow and C. E. Levy. Wheelchair propulsion biomechanics and wheelers' quality of life: an exploratory review. *Disability and Rehabilitation: Assistive Technology*, 6(5): 365–377, 2011. ISSN 1748-3107. doi: 10.3109/17483107.2010.525290.

R. A. Cooper. Wheelchair racing sports science: A review. *Journal of Rehabilitation Research and Development*, 27(3):295, 1990. ISSN 0748-7711. doi: 10.1682/jrrd.1990.07.0297.

R. de Klerk, R. J. K. Vegter, H. E. J. Veeger, and L. H. V. van der Woude. Technical note: A novel servo-driven dual-roller handrim wheelchair ergometer. *IEEE Transactions on Neural Systems and Rehabilitation Engineering*, 28(4):953–960, 2020. doi: 10.1109/TNSRE.2020.2965281.

W. H. K. de Vries, R. M. A. van der Slikke, M. P. van Dijk, and U. Arnet. Real-life wheelchair mobility metrics from imus. *Sensors*, 23(16), 2023. ISSN 1424-8220. doi: 10.3390/s23167174. URL https://www.mdpi.com/1424-8220/23/16/7174.

X. io Technologies. Second generation imu for real-time wireless and data logging applications, 2024. URL https://x-io.co.uk/NGIMU/. Last accessed 24 June 2024.

T. K. Koo and M. Y. Li. A guideline of selecting and reporting intraclass correlation coefficients for reliability research. *Journal of chiropractic medicine*, 15,2:155–63, 2016. doi: 10.1016/j.jcm.2016.02.012.

S. O. H. Madgwick. An efficient orientation filter for inertial and inertial / magnetic sensor arrays. 2010. URL https://api.semanticscholar.org/CorpusID:2976407.

K. O. McGraw and S. P. Wong. Forming inferences about some intraclass correlation coefficients. *Psychological Methods*, (1(1)):30–46, 1996. doi: https://doi.org/10.1037/1082-989X.1.1.30.

F. Pedregosa, G. Varoquaux, A. Gramfort, V. Michel, B. Thirion, O. Grisel, M. Blondel, P. Prettenhofer, R. Weiss, V. Dubourg, J. Vanderplas, A. Passos, D. Cournapeau, M. Brucher, M. Perrot, and E. Duchesnay. Scikit-learn: Machine learning in Python. *Journal of Machine Learning Research*, 12:2825–2830, 2011.

D. J. Sanderson and H. J. Sommer. Kinematic features of wheelchair propulsion. *J Biomech.*, 18(6):423–429, 1985. doi: 10.1016/0021-9290(85)90277-5.

R. Vallat. Pingouin: statistics in python. *Journal of Open Source Software*, 3(31):1026, 2018. ISSN 2475-9066. doi: 10.21105/joss.01026.

L. H. van der Woude, D. J. Veeger, R. H. Rozendal, and T. J. Sargeant. Seat height in handrim wheelchair propulsion. *Journal of rehabilitation research and development*, 26(4): 31–50, 1989.

L. H. V. Van Der Woude, H. E. J. Veeger, R. H. Rozendal, and A. J. Sargeant. Optimum cycle frequencies in hand-rim wheelchair propulsion. *European Journal of Applied Physiology and Occupational Physiology*, 58(6):625–632, 1989. ISSN 0301-5548. doi: 10.1007/bf00418509.

H. E. J. Veeger, L. H. V. Van Der Wouden, and R. R. H. Within-cycle characteristics of the wheelchair push in sprinting on a wheelchair ergometer. *Medicine Science in Sports Exercise*, 23(2):264–271, 1991.

G. A. Wolfe, R. Waters, and H. J. Hislop. Influence of Floor Surface on the Energy Cost of Wheelchair Propulsion. *Physical Therapy*, 57(9):1022–1027, 09 1977. ISSN 0031-9023. doi: 10.1093/ptj/57.9.1022. URL https://doi.org/10.1093/ptj/57.9.1022.

V. Yves, T. Daniel, and D. Dan. Wheelchair propulsion biomechanics. *Sports Medicine*, 31 (5):339–367, 2001. ISSN 0112-1642. doi: 10.2165/00007256-200131050-00005.

Chapter 5

Appendix

```python
def decode_data(df1):
    for j in range(24):
        df1[f"el{j+1}"] = range(len(df1["Data"]))


    for i in range(len(df1["Data"])):
        df1["Data"][i] = df1["Data"][i][2:-4] + '000'

        for j in range(24):
            a = df1["Data"][i][j*8 : j*8+7]
            b = f"{a[1]}{a[3]}{a[5]}"
            df1[f"el{j+1}"][i] = b

    df1 = df1.drop('Data', axis=1)
    df1.rename(columns={'el1': 'el5', 'el5': 'el1'}, inplace=True)
    df1 = df1.astype(float)
    df1.iloc[:, 1:] = df1.iloc[:, 1:] - df1.iloc[1, 1:]
    return df1
```

Listing 5.1: Code used to read electrode values from one measurement.

```python
# ---------------------------------------------------------------- #
    # function that is ran per push and
    #   (1) detects if the push seems valid,
    #   (2) detects if it is only 1 push &
    #   (3) returns the push electrode
# ---------------------------------------------------------------- #

def get_local_frame(push_aux):
    th = 1 #threshhold for the sum value
    mask = push_aux.keys()[:24]
    temp_sum = push_aux[mask].sum()
    temp_sum.index = np.linspace(1,24,24)
    n_largest = temp_sum.nlargest(4)


# detect 'No Push (NP)' touch
# ---------------------------------------------------------------- #
```

```
18       if n_largest.iloc[0] < th:
19           return 'NP' #return no push
20

21
22 # case with only 1 clear touch indication
23 # ---------------------------------------------------------------- #
24       elif n_largest.iloc[1] < th:
25           return str(n_largest.index[0]) #return electrode
26
27 # check if the two most touched electrodes are next to eachother
28 # ---------------------------------------------------------------- #
29       if abs(n_largest.index[0] - n_largest.index[1]) == 1:
30
31           #situation where n_largest.iloc[1] >>> n_largest.iloc[2]
32           if abs(n_largest.iloc[1] - n_largest.iloc[2]) > th:
33               temp_el = n_largest.index[0] + (n_largest.index[1]
34                       - n_largest.index[0]) * n_largest.iloc[1]
35                       / (n_largest.iloc[1] + n_largest.iloc[0])
36               temp_el = np.round(temp_el,1)
37               return str(temp_el)
38           else:
39               return str(n_largest.index[0])
40

41
42 # check if the two most touched electrodes are (el1 and el24)
43 # ---------------------------------------------------------------- #
44       elif abs(n_largest.index[0] - n_largest.index[1]) == 23:
45
46           #situation where n_largest.iloc[1] >>> n_largest.iloc[2]
47           if n_largest.iloc[1] - n_largest.iloc[2] > th:
48               temp_el = n_largest.index[0] + ((n_largest.index[1]
49                       - n_largest.index[0]) / 23 ) * n_largest.iloc[1]
50                       / (n_largest.iloc[1] + n_largest.iloc[0])
51               temp_el = np.round(temp_el, 1)
52               return str(temp_el)
53           else:
54               return str(n_largest.index[0])
55
56 # case with 2 clear touch indication that are not next to each other
57 # ---------------------------------------------------------------- #
58       else:
59           return 'TT' #TT for two touches
```

Listing 5.2: Code used to identify different touch situations.

```
1 # ---------------------------------------------------------------- #
2 # function that returns quaternions per experiment that
3 # (1) relate to the angle closest to gravity but within the wheels plane
4 # (2) create an offset quaternion that calibraties the local frame to the
      global frame (on -30 degrees at the second touch if no video data is
      avaiable)
5 # ---------------------------------------------------------------- #
6
7 def calibrate_push_angles(file, offset):
```

```
8
9      # get closest quaternion time at the second push -> will be used to
    calibrate local frame to global
10     second_push = push[file]['push start'].iloc[2]
11     second_push_qs = get_closest_qs_time(i,second_push)
12
13     #global frame in the plane of the wheel
14     q_global = qs[file]['quat'].iloc[abs(qs[file]['Y']).argmin()] # find a
    global reference (not that interesting)
15
16     # which electrode has the highest signal at 'second_push'
17     '''This value needs to be found differently, not at the start of a
    push'''
18     temp_angle = float(push[file]['el touch'].iloc[2]) - 1 # needs the -1
19     q_loc =  Quaternion(axis=[0.0, 1.0, 0.0], degrees = 15 * temp_angle)
20
21     # find quaternion of the global frame at the second push
22     q_second_push = qs[file].loc[second_push_qs]['quat']
23
24     #define the 'calibration' touch angle and calculate the offset needed
25     q_cal = Quaternion(axis=[0.0, 1.0, 0.0], degrees = offset) #set to 30
    degrees from the top (150 from the bottom)
26
27     # rotation that should be added to make the second touch start at 150
    degrees
28     q_offset = q_cal * (q_loc * q_second_push * q_global.inverse).inverse
29
30     #q_tot = q_offset * local_frame[el_max] * q_second_push * q_global.
    inverse
31     #print(q_tot.degrees * q_tot.axis[1])
32
33     return q_global, q_offset
34
35 # ------------------------------------------------------------------- #
36 #   function that returns a touch and release angle per push
37 # ------------------------------------------------------------------- #
38
39 def get_touch_angles(file, q_global, q_offset):
40
41     touch_angle = []
42     release_angle = []
43
44     #get touch point
45     for index in push[file].index:
46         time = push[file]['push start'].iloc[index]
47
48         #get closest time
49         qs_time = get_closest_qs_time(i,time)
50
51         #get electrode with the max value
52         temp_angle = float(push[file]['el touch'].iloc[index]) - 1
53         q_loc = Quaternion(axis=[0.0, 1.0, 0.0], degrees = 15 * temp_angle
    )
54
```

```
55        # find quaternion global frame
56        q_push = qs[file].loc[qs_time]['quat']
57
58        # find the total orientation related to gravity
59        q_tot = q_offset * q_loc * q_push * q_global.inverse
60
61        touch_angle.append(q_tot.degrees * q_tot.axis[1])
62
63    #get touch point
64    for index in push[file].index:
65        time = push[file]['push stop'].iloc[index]
66
67        #get closest time
68        qs_time = get_closest_qs_time(file,time)
69
70        #get electrode with the max value
71        temp_angle = float(push[file]['el touch'].iloc[index]) - 1
72        q_loc = Quaternion(axis=[0.0, 1.0, 0.0], degrees = 15 * temp_angle
    )
73
74        # find quaternion global frame
75        q_push = qs[file].loc[qs_time]['quat']
76
77        q_tot = q_offset * q_loc * q_push * q_global.inverse
78
79        release_angle.append(q_tot.degrees * q_tot.axis[1]) #
80
81    return np.array(touch_angle), np.array(release_angle)
```
Listing 5.3: Functions used to calculate the touch/release quaternion.

Test	N_{RH}	N_V	τ_{RH} (s)	τ_V (s)	α_{RH} (°)	α_V (°)	β_{RH} (°)	β_V (°)
$S1R1_1$	70	69	.34 ± .09	.34 ± .07	-15 ± 11	-14 ± 7	57 ± 9	55 ± 6
$S1R1_2$	67	67	.33 ± .07	.35 ± .05	-36 ± 7	-36 ± 2	32 ± 7	38 ± 4
$S1R1_3$	63	63	.25 ± .10	.32 ± .07	-10 ± 11	-22 ± 5	44 ± 11	44 ± 5
$S2R1_1$	21	21	.18 ± .20	.20 ± .13	-9 ± 16	-13 ± 6	84 ± 28	91 ± 4
$S2R1_2$	20	19	.19 ± .22	.22 ± .18	-38 ± 30	-38 ± 8	48 ± 40	70 ± 4
$S2R1_3$	19	19	.16 ± .13	.18 ± .10	-23 ± 13	-18 ± 6	53 ± 15	74 ± 2
$S2R1_4$	22	22	.21 ± .35	.19 ± .12	-10 ± 24	-16 ± 11	80 ± 17	83 ± 3
$S1R2_1$	34	35	.40 ± .11	.42 ± .09	-50 ± 11	-32 ± 3	32 ± 8	52 ± 3
$S1R2_2$	64	64	.29 ± .10	.27 ± .08	-27 ± 10	-20 ± 4	37 ± 8	44 ± 5
$S1R2_3$	76	76	.31 ± .10	.31 ± .08	-11 ± 8	-13 ± 4	53 ± 7	51 ± 3
$S2R2_1$	19	21	.15 ± .15	.17 ± .13	-13 ± 25	-17 ± 7	59 ± 15	78 ± 3
$S2R2_1$	19	16	.21 ± .19	.21 ± .13	-36 ± 24	-32 ± 7	50 ± 15	61 ± 4

Table 5.1: Detected pushes (N), average push time per test (τ), average contact angle per test (α) & average release angle per test (β). Pushes are the total pushes in a test, the rest is notated into mean ± standard deviation. RHIDE results have the subscript 'RH' and video results have the subscript 'V'.